Extraction of Open-Loop Frequency Response of Power Apparatus using Transient Data from Multiple Naturally Occurring Disturbances

Santosh V. Singh, A. M. Kulkarni and H. J. Bahirat

***Abstract*—Frequency response analysis (FRA) is a mature technique to characterize the behaviour of apparatus like transformers, and is commonly used for condition monitoring and diagnostics. FRA is also used for sub-synchronous resonance/control interaction analysis of rotating machines and power electronic converters. The frequency responses (transfer functions) can be experimentally obtained from tests at the apparatus terminals. These are generally done offline, i.e. when the equipment is out of service. Online testing is attractive as it can be done frequently and periodically, but it requires auxiliary equipment for injecting probing signals into an energized high voltage system. The alternative online approach uses high bandwidth measurements of "naturally" occurring external transients (due to faults, switching and other disturbances) to obtain the frequency response. The key challenge in online FRA of multi-port apparatus is in the extraction of the "open-loop" transfer function of the apparatus, while connected to the rest of the system, essentially in a "closed-loop" configuration. This paper proposes a technique to address this challenge by utilizing data from multiple independent events, and presents proof-of-concept simulations. The technique can be applied not only to passive components like transformers and transmission lines, but also to power electronic systems and rotating machines.**

***Keywords*—Frequency Response Analysis, least square technique, zero-phase digital filtering, frequency scanning.**

I. Introduction

FREQUENCY Response Analysis (FRA) is a model extraction technique which is used for condition monitoring and diagnostics, and grid interaction analysis of power apparatus and systems. Since the parameters that affect the dynamic behaviour (for example, the capacitances) depend on material properties and the geometric configuration of conductors and other components, any changes in the properties or configuration can be detected by tests and measurements, done regularly or after major events. This is the basis for the use of FRA for condition monitoring and diagnostics of apparatus like power transformers [1], [2], [3], [4], [5]. The frequency responses are also used in screening tools for sub-synchronous resonance (SSR), sub-synchronous control interactions (SSCI) and harmonic instabilities [6], [7], [8] associated with rotating machines, power electronic systems and their associated controllers.

S. V. Singh, A. M. Kulkarni and H. J. Bahirat are with Electrical Engineering Department of Indian Institute of Technology Bombay, Mumbai-400076, INDIA (e-mail: santoshvsingh68@gmail.com, anil@ee.iitb.ac.in, hjbahirat@ee.iitb.ac.in).

Paper submitted to the International Conference on Power Systems Transients (IPST2021) in Belo Horizonte, Brazil June 6-10, 2021.

The FRA approach in its original form is an offline method, where the apparatus is taken out from service, i.e. disconnected from the network. The apparatus is excited with an externally generated signal, and the input and outputs are processed to obtain the transfer functions. Multi-sine, chirp and low voltage impulses are examples of signals that have been used for FRA. The spectrum of the signal is chosen such that it has adequate bandwidth and resolution so as to capture the modal frequencies of interest.

Online FRA is a variant of this technique, which involves measurements taken at the apparatus terminals while the apparatus is still in operation. The advantage of online FRA is that condition monitoring can be done at regular and frequent intervals without requiring equipment outage. Online FRA can be categorized into two methods:

Method 1: Probing signals (like the ones used for offline FRA) are injected at the terminals using a signal generator and coupling equipment [1], [9].

Method 2: The transient behaviour following naturally occurring external disturbances, like lightning, faults and switching, are used to obtain the frequency response [10], [11], [12].

In the online methods, the measured frequency responses for three-phase multi-port apparatus are, in fact, those of the "closed loop" transfer functions that correspond to the apparatus embedded in rest of the system. The closed loop transfer functions are affected by the parameters and topology of the external network. These may be quite different from the "open loop" (individual) transfer functions of the apparatus, which are required in most applications, including condition monitoring. The extraction of the open-loop transfer functions with online methods has not been satisfactorily addressed in the previous literature. This paper proposes a method to achieve this using measurements from multiple transient events. The open-loop frequency response is obtained as a least squares solution to an over-determined set of equations corresponding to the measurements.

The proposed technique can be applied to obtain the frequency response of transformers, three-phase transmission lines and cables, power electronic systems and rotating machines. Since the frequency response is meaningful when the system is time-invariant, the estimation is done using D-Q-o variables (synchronously rotating frame of reference) in the case of power electronic systems and rotating machines. In the case of transmission lines, the time synchronization of

the measurements at both ends of a transmission line or a cable is feasible using a Global Positioning System (GPS). FRA of transmission lines and cables can provide a validation of the theoretical frequency dependent models and parameters. This is of practical relevance for the accurate representation of these elements in transient simulation programs.

The paper presents simulation studies to demonstrate the utility of the proposed method in determination of frequency responses of transformer, transmission line, STATCOM and synchronous generator. Numerical experiments are performed to evaluate the effect of measurement resolution, the number of events and the use of transformed variables (Clarke's transformation). Note that the method requires high bandwidth measurements, data logging, communication and off-line signal-processing, which are well within the capabilities of currently available technologies.

II. The Proposed Method

In this section, we present a simple example to illustrate the computation of a transfer function using transient waveforms in a single-phase circuit. Thereafter, we consider the problem of obtaining the required ("open-loop") transfer function of multi-port three-phase apparatus using measurements from multiple transient events.

A. FRA using Transient Waveforms

Consider a single-phase circuit as shown in Fig. 1. The parameters of the circuit are R_s = 0.1 Ω, R_e = 0.2 Ω and L_e = 2 mH. The admittance transfer function $Y(j\omega)$ corresponds to a series RLC circuit with the parameters R_r = 2 Ω, L_r = 10 mH and C_r = 20 μF respectively. The source voltage is $v_s(t) = 10\,\sin(2\,\pi \times 50\,t)$ V.

The system is initially in steady-state. At t_1 = 0.484 s, there is a short circuit due to closing of the switch as indicated in the circuit. The breakers a and b opened, isolating one of the parallel links at t_2 = 0.488 s. The measured voltage and current waveforms, $v_r(t)$ and $i_r(t)$, are shown in Fig. 1.

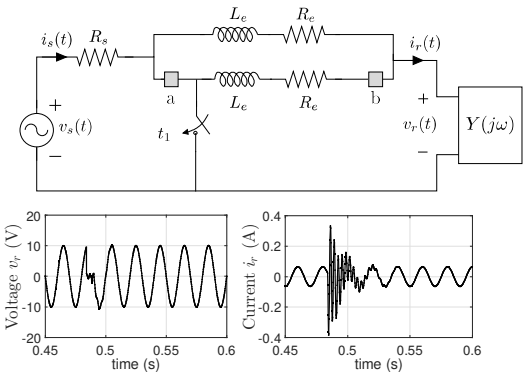

Fig. 1. A single-phase circuit, and the measured transient waveforms.

The signal processing required to obtain the transfer function $Y(j\omega)$, is depicted in Fig. 2. Note that,

1) An analog high pass filter is used to remove the 50 Hz component in the waveforms, and isolate the transient components. This is done so that the resolution of the analog-to-digital converter (ADC) that follows is utilized for representing the transient component, and is not swamped out by the 50 Hz component.

2) Once the digital signals (voltage and current) are obtained, further processing is carried out on the record that encompasses the transient till it practically becomes zero. The record is effectively a *time-limited* signal i.e., it is non-zero over a finite duration only. Therefore, the ratio of Discrete Fourier Transform (DFT) of the current and voltage samples in this record directly gives us the transfer function $Y(j\omega)$.

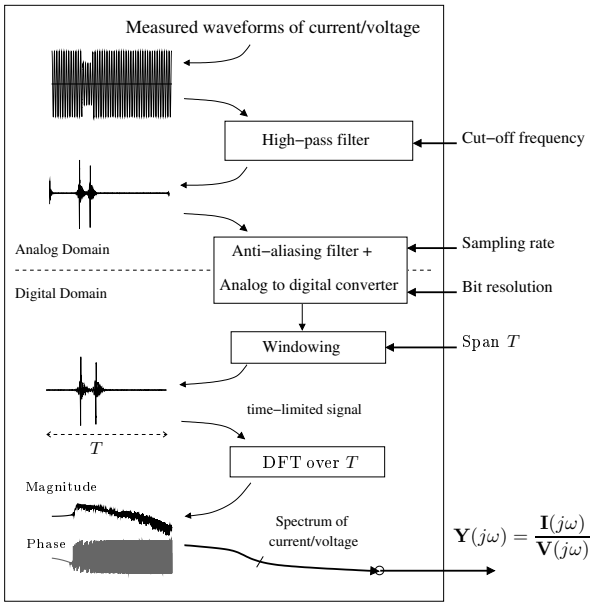

Fig. 2. Signal processing steps for Online FRA estimation using transient waveforms.

We apply this procedure to the transient waveforms shown in Fig. 3, which are obtained by simulating the system using a time step of 1 μs. A fifth order high-pass analog Butterworth filter with a cut-off frequency 200 Hz is used. The time duration of the sample record is 0.9 s (from 0.01 s to 0.91 s), while the sampling rate is 20 kHz, obtained by down-sampling the simulation data. The filtered current and voltage waveforms, the DFT of these signals, and the transfer functions are shown in Fig. 3. Overall, there is a good match between estimated admittance $Y_{estimated}$ and the actual admittance Y_{actual}, as indicated in Fig. 4. At lower frequencies, however, some distortions are seen. These are not surprising because the high pass filter significantly diminishes the frequency components at lower frequencies resulting in poorer numerical conditioning in that range.

B. Application to Three-Phase Apparatus

At first glance, obtaining the frequency response of a single or multi-port three-phase apparatus while it is in operation seems to be a straight-forward extension of the method depicted in Fig. 2. However, a closer inspection reveals some complexities. To understand this, consider a three-phase two-port apparatus connected to the rest of this system, as shown in Fig. 5. For a disturbance occurring in the power system, twelve terminal variables (six voltages and six currents) can be measured as shown. Using the procedure

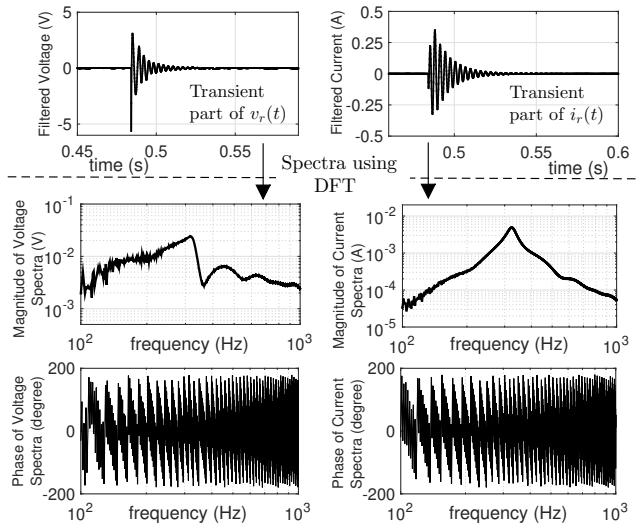

Fig. 3. Spectra over a time window for transient parts of $v_r(t)$ and $i_r(t)$.

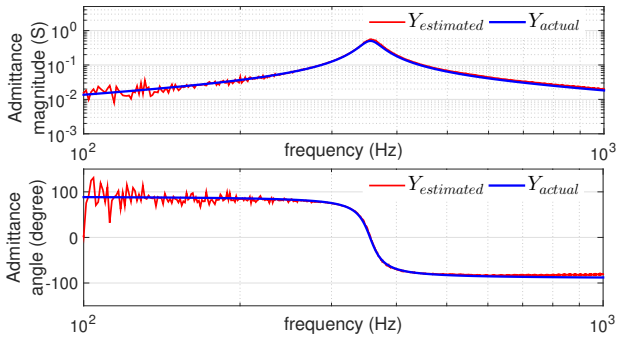

Fig. 4. Admittance $Y(j\omega)$ for the Fig. 1 circuit.

shown in Fig. 2, the spectrum of these variables can be obtained.

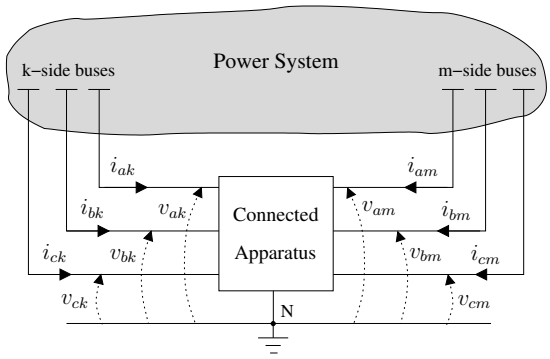

Fig. 5. Three-phase two port apparatus connected to rest of the system.

The multi-port admittance (or impedance) transfer function of this apparatus is a 6×6 matrix, as shown in (1).

$$\mathbf{I}(j\omega)_{6\times1} = \mathbf{Y}(j\omega)_{6\times6}\,\mathbf{V}(j\omega)_{6\times1} \tag{1}$$

where,

$\mathbf{I}(j\omega) = [I_{ak}(j\omega)\ \ I_{bk}(j\omega)\ \ I_{ck}(j\omega)\ \ I_{am}(j\omega)\ \ I_{bm}(j\omega)\ \ I_{cm}(j\omega)]^{\mathrm{T}}$

$\mathbf{V}(j\omega) =$

$[V_{ak}(j\omega)\ \ V_{bk}(j\omega)\ \ V_{ck}(j\omega)\ \ V_{am}(j\omega)\ \ V_{bm}(j\omega)\ \ V_{cm}(j\omega)]^{\mathrm{T}}$

$$\mathbf{Y}(j\omega) = \begin{bmatrix} Y_{ak-ak}(j\omega) & \cdots & Y_{ak-cm}(j\omega) \\ \vdots & \ddots & \vdots \\ Y_{cm-ak}(j\omega) & \cdots & Y_{cm-cm}(j\omega) \end{bmatrix}$$

$\mathbf{Y}(j\omega)$ represents the *open-loop* admittance matrix of the apparatus. Since the matrix $\mathbf{Y}(j\omega)$ is symmetric, the number of distinct admittance elements to be estimated is 21. The relation (1) can be rearranged as (2).

$$\mathbf{I}(j\omega)_{6\times1} = \mathbf{V_e}(j\omega)_{6\times21}\,\mathbf{Y_e}(j\omega)_{21\times1} \tag{2}$$

where, $\mathbf{V_e}(j\omega)$ is a matrix composed of the elements of $\mathbf{V}(j\omega)$, and $\mathbf{Y_e}(j\omega)$ is a column matrix composed of the upper triangular elements of $\mathbf{Y}(j\omega)$.

No unique solution exists for (2) since the unknowns (21) exceed the number of equations (6). This problem can be overcome by considering measurements for multiple events. To estimate 21 distinct admittance elements, at least 21 distinct equations are required. For an event, only 6 relations are available -see (1). Therefore with a minimum of four events it is possible, in principle, to obtain the required admittance matrix elements. The assumption is that the events are distinct, have a high signal-to-noise ratio, and are "spectrally rich", i.e., they have adequate amplitudes for different frequencies in the range of interest. Consideration of a larger number of events is beneficial from this perspective. The solution of the over-determined set of equations in (3) can then be obtained using the least squares technique.

$$\begin{bmatrix} \mathbf{I_1}(j\omega)_{6\times1} \\ \vdots \\ \mathbf{I_N}(j\omega)_{6\times1} \end{bmatrix} = \begin{bmatrix} \mathbf{V_{1e}}(j\omega)_{6\times21} \\ \vdots \\ \mathbf{V_{Ne}}(j\omega)_{6\times21} \end{bmatrix} \mathbf{Y_e}(j\omega)_{21\times1} \tag{3}$$

The overall approach is depicted in Fig. 6. Note that for a single-port three-phase apparatus, the number of unknowns is 9, requiring a minimum of 3 independent events.

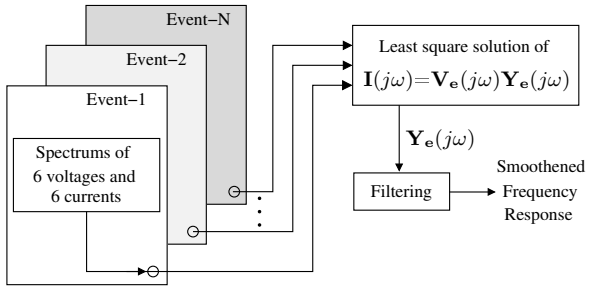

Fig. 6. Least square solution for FRA estimation using N-events.

C. Estimation in α-β-o variables

The least squares estimation may alternatively be done using the α-β-o variables obtained by Clarke's transformation, which is defined as follows:

$$\begin{bmatrix} f_a \\ f_b \\ f_c \end{bmatrix} = T_c \begin{bmatrix} f_\alpha \\ f_\beta \\ f_o \end{bmatrix},\ T_c = \sqrt{\frac{2}{3}} \begin{bmatrix} 1 & 0 & \frac{1}{\sqrt{2}} \\ -\frac{1}{2} & -\frac{\sqrt{3}}{2} & \frac{1}{\sqrt{2}} \\ -\frac{1}{2} & \frac{\sqrt{3}}{2} & \frac{1}{\sqrt{2}} \end{bmatrix}$$

The admittances in the (a-b-c) and (α-β-o) reference frame are related by a similarity transformation. For a single-port three-phase apparatus, this may be expressed as

$Y_{\alpha\beta o} = T_c^{-1} Y_{abc} T_c$. The formulation of the least square problem is the same as (2), except that the phase measurements are first transformed, and then the transformed admittance is estimated, from which the phase-domain admittance can be recovered. The least square solution in the Clarke's variables is essentially the same, as the transformation is orthogonal ($T_c^{-1} = T_c^T$). However, from a computational viewpoint, the transformation of variables may improve the numerical conditioning. Note that the admittance matrix in α-β-o variables is known to be diagonal dominant even if a slight unbalance is present.

D. Frequency Response of Power Electronic Converters and Rotating Machines

Power electronic converters and rotating machines have to be handled in a manner different from passive components like transformers and transmission lines. This is because the underlying model in the (a-b-c) or (α-β-o) variables is not time invariant and could also be non-linear. FRA is meaningful only for linear time-invariant systems. Hence the small-signal (linear) models may be estimated by considering only small disturbances in the estimation process. Moreover, only the set of disturbances around similar operating conditions should be considered to obtain a model corresponding to those conditions.

To achieve time-invariance, a synchronously rotating (D-Q-o) transformation of variables may be used[1], as given below.

$$[f_a \;\; f_b \;\; f_c]^T = C_p(\gamma)\,[f_D \;\; f_Q \;\; f_o]^T \tag{4}$$

where

$$C_p(\gamma) = \sqrt{\frac{2}{3}} \begin{bmatrix} \cos(\alpha) & \sin(\alpha) & \frac{1}{\sqrt{2}} \\ \cos(\alpha - \frac{2\pi}{3}) & \sin(\alpha - \frac{2\pi}{3}) & \frac{1}{\sqrt{2}} \\ \cos(\alpha - \frac{4\pi}{3}) & \sin(\alpha - \frac{4\pi}{3}) & \frac{1}{\sqrt{2}} \end{bmatrix}$$

and $\alpha = \omega_o t + \gamma$. The frequency ω_o and the angle γ are constants. The frequency ω_o is chosen to be the steady state operating frequency. The admittance matrix is estimated in this frame of reference [7], the procedure being the same as in the case of phase domain variables. Since γ will affect the individual terms of the admittance matrix in the D-Q-o variables [13], it has to be chosen in a consistent manner. It is convenient to choose γ such that the pre-disturbance quiescent 'D' component of the terminal voltage is zero.

III. Case Study-I: Transformer and Transmission Line

A. System Description

Fig. 7 shows a time-domain EMTP-ATP simulation model of a portion of the transmission network of an Indian utility. The system has several 220 kV, 400 kV and 765 kV transmission lines, interconnected using transformers. The rest of the system is represented as a multi-port Thevenin equivalent at the boundary buses. The timestep for simulation is Δt = 1 μs and simulation duration is T = 1 s.

[1]For power electronic systems, it is assumed that the effect of switching harmonic components are negligible at the point of connection with the grid.

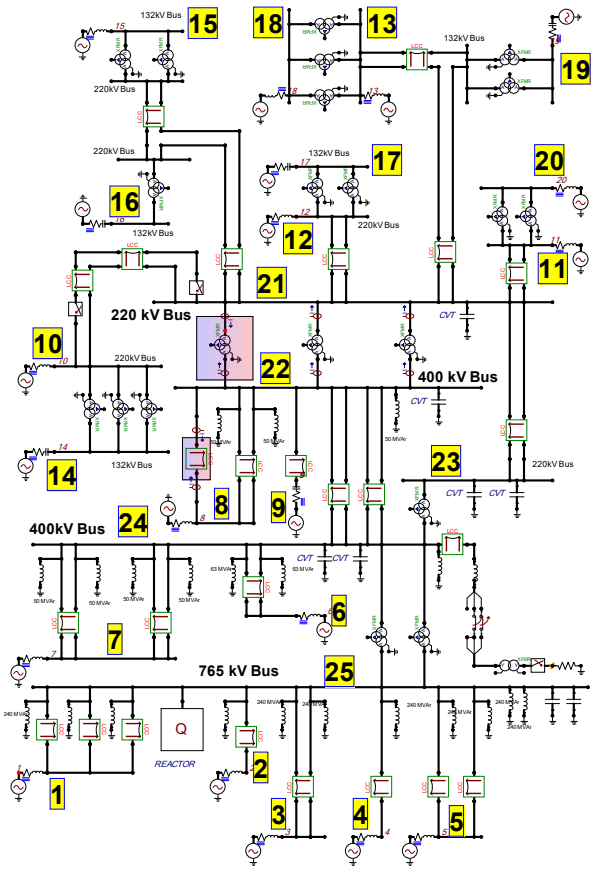

Fig. 7. EMTP-ATP model of the Transmission System.

1) Three-phase auto-transformer model: A 315 MVA, 400 kV/ 220 kV, 50 Hz wye-wye auto-transformer with grounded neutral, connected between bus-21 and bus-22, is used to demonstrate the proposed technique. A hybrid model [14] is used as shown in Fig. 8, with typical values of capacitances [2]. The hybrid model is also appended with a set of resonant circuit blocks, which introduces high frequency resonant modes when observed from the terminals.

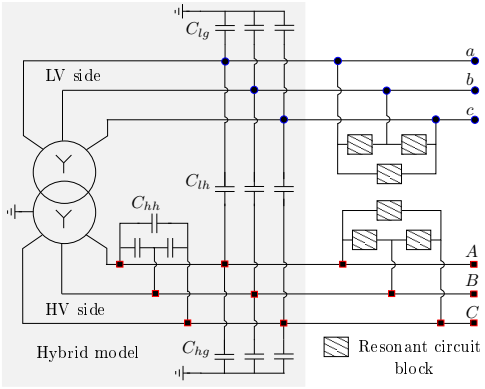

Fig. 8. Modified three-phase auto-transformer model used in the simulation.

The resonant circuit blocks are constructed using RLC elements, the parameters for which are calculated from the desired resonant frequency and the quality factor [15].

2) Three-phase overhead transmission line model: The single-circuit 200 km, 400 kV three-phase

overhead transmission line connected between bus-8 and bus-22 is considered for online FRA estimation. The frequency-dependent EMTP-ATP model of the transmission line is used [16]. The standard tower and line specifications are obtained from [17] for 400 kV.

TABLE I
SYSTEM DISTURBANCES USED FOR ONLINE FRA ASSESSMENT

Sr. No.	Distance† (km)	Description of events (Short circuit fault)	Event after fault	Clearing time (ms)
1	7	a-phase to ground	3-phase line trip	80
2	13	c-phase to ground	c-phase line opening	55.5
3	20	ab-phases to ground	3-phase line trip	80
4	32	a-phase to ground	3-phase line trip	67.5
5	37	bc-phases to ground	3-phase line trip	55.5
6	40	b-phase to ground	3-phase line trip	80
7	44	ab-phases to ground	3-phase line trip	67.5
8	50	ac-phase to ground	3-phase line trip	68
9	50	c-phase to ground	c-phase line opening	45
10	52	c-phase to ground	c-phase line opening	96
11	57	a-phase to ground	a-phase line opening	96
12	70	c-phase to ground	3-phase line trip	67.5
13	80	a-phase to ground	3-phase line trip	68.5
14	92	b-phase to ground	b-phase line trip and reclosure	53 96*
15	100	b-phase to ground	b-phase line trip and reclosure	45 364*
16	120	a-phase to ground	3-phase line trip	340
17	125	c-phase to ground	3-phase line trip	67.5
18	0.73	abc-phases	3-phase line trip	250
19	0.73	abc-phases	3-phase line trip	250

† Distance in km from k-side (bus-22 in Fig. 7) terminal of the unit
* Time taken from clearing time to the reclosure action.

For accurate estimation, a diverse set of disturbance events are required. Table I shows the list of credible events which are used for this case study. The signal processing steps indicated in Figs. 2 and 6 are used for the estimation. Note that a smoothening filter is applied at the last step, as shown in Fig. 6. This is done in order to remove the distortions in the frequency response caused by low amplitudes of the signals at certain frequencies which were seen in the unfiltered estimates of the transfer functions at the lower frequencies (see Fig. 4).

In the present case study, filtering is done by passing the frequency (ω) versus complex $\mathbf{Y_e}(j\omega)$ data through a zero-phase low pass filter `filt-filt` of MATLAB [18]. Table II gives the details of the parameters used in the study. The estimation is done in the range 400 Hz - 150 kHz for the transformer, and 400 Hz - 5 kHz for the transmission line.

TABLE II
SIGNAL PROCESSING PARAMETERS FOR ONLINE FRA ESTIMATION

Sr. No.	Attributes	Parameters: Transformer Case	Parameters: Transmission Line Case
1	ADC specifications		
	Bipolar resolution	12 bit (default)	12 bit (default)
	Peak Transient Voltage*	55 kV	60 kV
	Peak Transient Current*	1000 A	250 A
2 (See Fig. 6)	Zero phase filtering of $\mathbf{Y_e}$	Low-pass	Low-pass
	Stopband frequency	0.002 Hz	0.08 Hz
	Stopband Attenuation	60 dB	60 dB
	Passband frequency	0.0005 Hz	0.04 Hz
	Passband Attenuation	1 dB	1 dB

* These are the values (referred to the high voltage side of the instrument transformer) that the ADC can capture within its range.

B. FR estimation of Transformer

It is observed that with four events singularities are obtained at certain frequencies. These singularities result from inadequate spectral richness in the set of four events. With nine events and the 12-bit ADC, the admittance matrix for the transformer is estimated. An element Y_{ak-ak} is shown in Fig. 9. The actual admittance matrix is denoted by Y_{actual}. Note that the unfiltered estimate is noisy as indicated by $Y_{est-noisy}$. It is filtered using the zero-phase filter which was discussed earlier, to provide a smoother response, $Y_{estimated}$. The accuracy of the proposed technique with respect to the measured response is evaluated using root mean square error (RMSE) which is calculated as RMS value of ($Y_{actual} - Y_{estimated}$) in the given frequency range.

The actual and estimated transfer functions seem to match reasonably well. It is observed from the figure that a larger deviation is obtained in the lower frequency range. The first resonance point occurs at a slightly lower frequency than the actual. A noticeable error occurs in the peak admittance value at the second resonance, which may be the side effect of smoothening the distortion in the raw estimates.

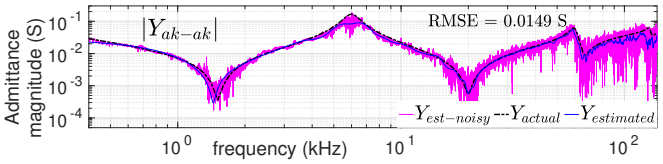

Fig. 9. Transformer admittance, Y_{ak-ak} using nine events and 12-bit ADC.

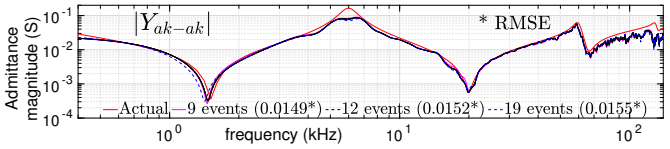

Fig. 10. Effect of number of events on the estimate for 12 bit ADC.

Fig. 10 shows a comparison of the FRA estimated using nine, twelve and nineteen events, which provides RMSE of 0.0149 S, 0.0152 S and 0.0155 S respectively. The number of events do not seem to impact the estimate significantly. It is possible that the nature of events may have a larger impact on the accuracy of estimate. A more diverse set of disturbances will give greater spectral richness, but the precise characterization of this set requires further study.

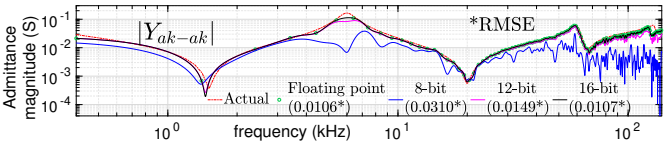

Fig. 11. Effect of number of ADC bits on the estimate for nine event case.

Fig. 11 shows the impact of ADC bit resolution. As the number of bits increases the RMSE reduces. Thus, increase in number of bits is expected to improve accuracy of estimate and also indicates that the errors reported in Figs. 9 and 12 may be due to low number of bits used in voltage and current measurements. It is expected that the sampling rate of ADC may also affect the accuracy of the estimation in higher frequency ranges of the FRA.

Fig. 12 shows plots for some other elements of the admittance matrix. The trend and resonant frequencies for the self and mutual terms are similar to the actual values. However, there are significant distortions in the higher frequency range. In the case of the mutual inductance between the primary and

secondary windings (Y_{ak-am}), higher error is obtained when capturing resonant frequency in the mid-frequency range. The relatively low value of this admittance may be correlated to this behaviour, but it requires further investigation.

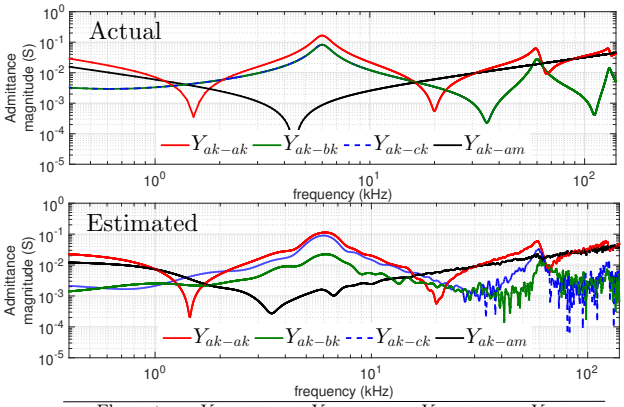

Element :	Y_{ak-ak}	Y_{ak-bk}	Y_{ak-ck}	Y_{ak-am}
RMSE (S) :	0.0107	0.0078	0.0068	0.0084

Fig. 12. Transformer admittances, Y_{abc} using nine events and 16-bit ADC.

1) Estimation in a-b-c variables: The matrix Y_e consists of 21 distinct elements. For brevity, only a few elements from the estimated admittance matrix are presented here. Based on the discussion in Section II-B, four events should suffice to calculate the required 21 distinct admittance elements. However, in order to improve accuracy as well to reduce impact of the noise more number of events are required.

2) Estimation in α-β-o variables: The transformer admittance, $Y_{\alpha\beta o}$ are shown in Fig. 13. The estimates are obtained using nine events, and 16-bit resolution is used for the data acquisition. The RMSE of the frequency responses are also indicated in the same figure. It can be seen that the estimated frequency responses match quite well with the actual frequency responses. The phase domain admittance Y_{abc} can be calculated from $Y_{\alpha\beta o}$.

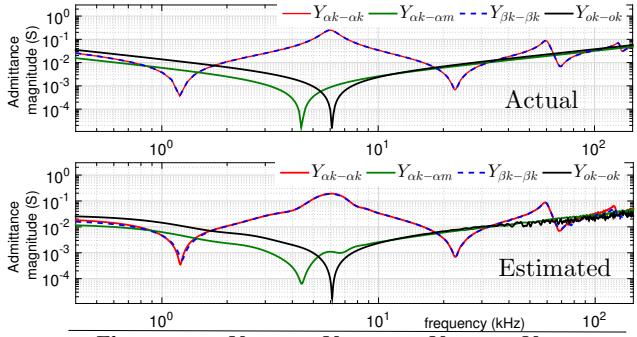

Elements :	$Y_{\alpha k-\alpha k}$	$Y_{\alpha k-\alpha m}$	$Y_{\beta k-\beta k}$	Y_{ok-ok}
RMSE (S):	0.0121	0.0034	0.0149	0.0137

Fig. 13. Transformer admittances, $Y_{\alpha\beta o}$ using nine events and 16-bit ADC.

C. FR estimation of Transmission Line

1) Estimation in abc variables: Using nine events and 16-bit ADC resolution, the admittance matrix of the transmission line is estimated. Few elements of the admittance matrix are shown in Fig. 14. It is observed that the nature of the variation is captured reasonably well for the diagonal and off-diagonal elements of the matrix. The effect of the number of events and ADC bits are seen to be similar to the observations with transformers.

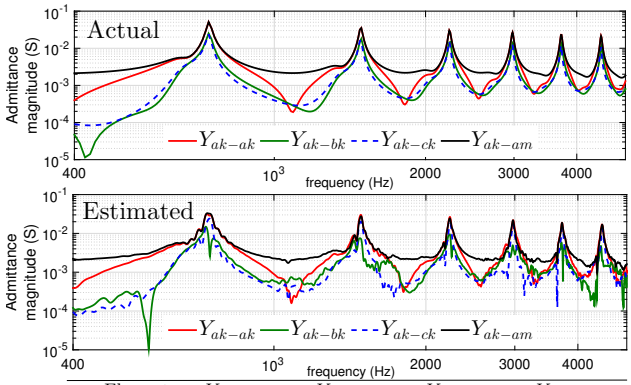

Element :	Y_{ak-ak}	Y_{ak-bk}	Y_{ak-ck}	Y_{ak-am}
RMSE (S) :	0.0015	0.0022	0.0012	0.0015

Fig. 14. Transmission line admittances, Y_{abc} using nine events and 16-bit ADC.

Unlike in the case of transformers, the measurements for the transmission line need to be time synchronized using GPS timestamps. It is observed that a typical time synchronization error of around 1 μs does not result in significant error for the frequency range of estimation that is considered here.

2) Estimation in α-β-o variables: The transmission line admittance, $Y_{\alpha\beta o}$ is shown in Fig. 15. The estimates are obtained using nine events, and 16-bit resolution is used for the data acquisition. The estimated frequency responses match quite well with the actual frequency responses. The admittance matrix Y_{abc} can be calculated from $Y_{\alpha\beta o}$.

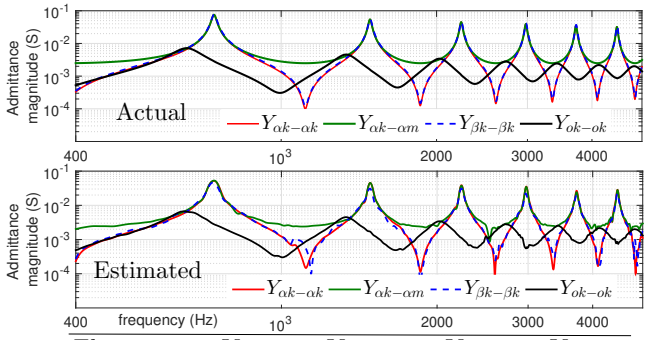

Elements :	$Y_{\alpha k-\alpha k}$	$Y_{\alpha k-\alpha m}$	$Y_{\beta k-\beta k}$	Y_{ok-ok}
RMSE (S):	0.0019	0.0021	0.0039	0.0002

Fig. 15. Transmission line admittances, $Y_{\alpha\beta o}$ using nine events and 16-bit ADC.

IV. Case Study-II: STATCOM

STATCOM is a VSC based device used for reactive power compensation [19]. The control system of a STATCOM consists of ac terminal voltage and dc voltage regulators which set the reference values of fast-acting inner current regulators. To reduce harmonics a sine-triangle PWM scheme is utilized.

In this study, a $\pm$200 MVAr STATCOM regulates the mid-point voltage of a 400 km, 500 kV transmission line as shown in Fig. 16. The FR of the STATCOM admittance (in D-Q-o variables) has been estimated using transient waveforms due to multiple disturbances at S. The

transient measurements are done at the point M in the figure. The time-step for the simulation is $\Delta t = 10$ μs which is down-sampled to 250 μs and simulation duration is $T = 5$ s. To ensure linearity, disturbances are applied at the remote end S, such that the magnitudes of the voltage and current deviations at the STATCOM bus are not very large.

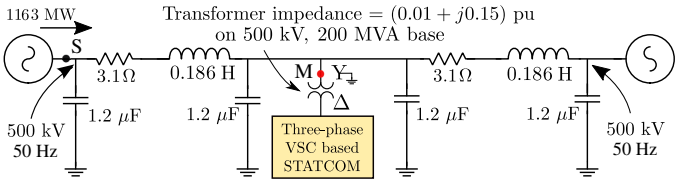

Fig. 16. System used for simulating the STATCOM case.

The actual frequency response of the STATCOM (at the same operating condition) is now separately extracted using numerical frequency scanning [7], [20].

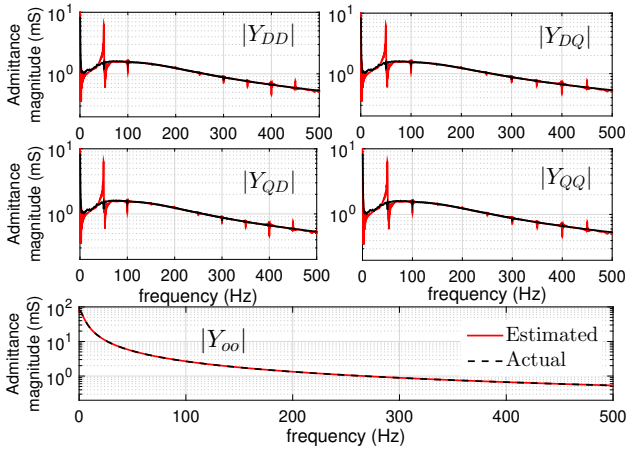

Fig. 17. Estimated frequency response of the STATCOM admittance matrix.

The STATCOM admittance in D-Q-o domain (obtained from transient waveforms) are given in Fig. 17. These frequency responses match quite well with the actual Y_{DQo} (also shown in Fig. 17). The deviations are higher near multiples of 50 Hz due to the presence of small, but non-zero harmonic components, as well as a very poorly damped mode at 50 Hz due to the transformer magnetizing reactance [21]. The zero-sequence admittance is decoupled from the D-Q components due to the star-delta connection and consists of only the leakage of the transformer.

V. Case Study III: Synchronous Generator

Consider the system shown in Fig. 18. The parameters of the generator and multi-mass turbine model are taken from the IEEE First Benchmark Model for SSR in [22]. A uniform modal damping of 5 % has been chosen for all the torsional modes. The parameters of the AVR, PSS and the quiescent values of power flow and terminal voltage are indicated in the figure. The transient measurements are done on the line side of the transformer (at the point M). The system has five torsional modes of which one is not observable in the electrical network [23], and one low frequency 'swing mode'. These are indicated by 0-4 in the figure. Note that in a synchronous machine there is a lightly damped mode due to the stator winding which has a rate of decay determined by the armature time constant. This is manifested as a mode at 60 Hz in the D-Q-o frame, as is seen in the figure.

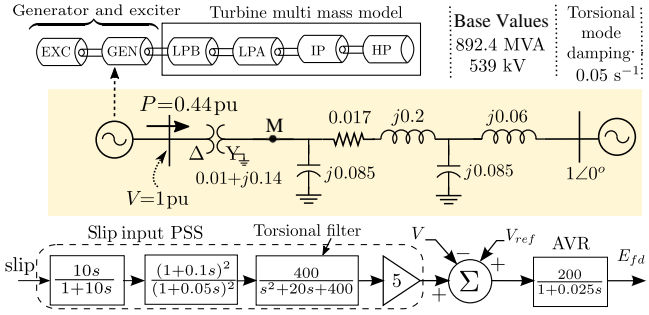

Fig. 18. System used for simulating the synchronous generator case.

The synchronous generator admittance Y_{DQo} has been estimated using transient waveforms due to multiple disturbances near the infinite bus. The time-step for the simulation is $\Delta t = 20$ μs which is down-sampled to 200 μs and simulation duration is $T = 100$ s. The disturbances are applied such that the magnitudes of the voltage and current deviations at M are not very large so that the linearized models can be extracted accurately.

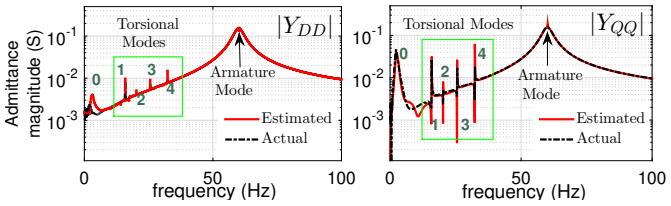

Fig. 19. Two components of the synchronous generator admittance.

The synchronous generator admittance Y_{DQo} (obtained from transient waveforms) are given in Fig. 19. The estimated frequency responses match quite well with the actual Y_{DQo} (also shown in Fig. 19).

VI. Discussion

(1) The proposed approach excludes the effect of network "feedback" on the transfer function, even though the apparatus is connected to the live network. Only the apparatus transfer function matrix is estimated, which is of interest for modelling and diagnostics.

(2) The method assumes that the apparatus transfer function remains unchanged during the events which are used for the estimation. In general, the estimation is continually done; the latest estimation would consider the latest event and a certain number of events immediately preceding it. Thus, any changes in the estimates may be tracked for diagnostic purposes.

(3) The least square solution that is used here is computationally expensive, but this is not the critical issue here since the FRA estimation is not done in real time.

(4) The approach requires current and voltage measurement at the terminals of the apparatus. The transducers used should have a sufficient bandwidth, resolution and a linear response. Note that in online methods, the transducers are coupled to the apparatus, which is operating in a high voltage and high current environment. Alternatives to conventional current and

voltage transformers, like Rogowski Coils and Non Invasive Capacitors (NICs) may be considered [24] to ensure an adequate bandwidth. Analog-to-Digital Converters (ADCs) of sufficient bipolar resolution and sampling rate are also required in the measurement system.

(5) The occurrence of the events may be detected using voltage based triggering as adopted in most disturbance recorders [25]. A predefined interval of the data is continuously stored in a buffer of the measurement device. When the trigger is activated, the buffer data is sent to a permanent storage device for further processing. If the measurement devices are far apart (say, on both ends of a transmission line), then the recordings need to be synchronized and time-stamped using a GPS.

(6) The frequency response estimation requires some pre-processing steps, especially in the case of power electronic systems and rotating machines, as the underlying models are non-linear. The operating conditions can be divided into various ranges and estimation can be done for the different operating ranges. Only small disturbances that occur when the apparatus is operating in a particular range are used for estimation in that range. The choice of different operating ranges and classification of disturbances as small or large requires some engineering judgement about the extent of non-linearity present.

VII. Conclusions

In this paper, an online FRA estimation methodology is discussed and is shown to be applicable to any power system apparatus. The "open-loop" transfer function of an apparatus connected in "closed-loop" configuration with the network, is estimated using naturally occurring system disturbances. This is achieved by solving a least square problem. The paper shows that theoretically, a minimum of four independent system disturbances are required for online FRA estimation of a two-port, three-phase apparatus. In practice, more events are required for the estimation. The proposed approach is illustrated for a three-phase auto transformer and transmission line. It is shown that the mere inclusion of more events may not improve the accuracy of the estimation proportionally. It is observed from the results that increasing the number of ADC bits leads to better estimation of FRA. The transformer and transmission line FRA estimation of the off-diagonal elements have more error as compared to the diagonal elements. This problem is largely solved by performing the estimation in the transformed (α-β-o) variables which appears to improve the numerical conditioning.

The method can be extended to power electronic apparatus and rotating machines, using the D-Q-o transformation. This is demonstrated using case studies of a STATCOM and the multi-mass model of a turbine-synchronous generator system.

Overall, the method appears to be promising and viable, but it needs further refinements to achieve better accuracy. These include better filtering of the raw estimates and the characterisation of a sufficiently diverse set of disturbances that would yield accurate estimates in the frequency range of interest. This would need to be followed up by an experimental validation in the field.

References

[1] E. Gomez-Luna, G. A. Mayor, C. Gonzalez-Garcia, and J. P. Guerra, "Current status and future trends in frequency-response analysis with a transformer in service," *IEEE Trans. on Power Delivery*, vol. 28, no. 2, pp. 1024–1031, Apr. 2013.

[2] CIGRE Technical Brochure 577A, *Electrical transient interaction between transformers and the power system - Part 1: Expertise*, CIGRE JWG A2/C4.39, 2014.

[3] CIGRE Technical Brochure 812, *Advances in the interpretation of transformer Frequency Response Analysis*, CIGRE WG A2.53, 2020.

[4] *IEEE Guide for the Application and Interpretation of Frequency Response Analysis for Oil-Immersed Transformers*, IEEE Standard C57.149-2012, Mar. 2013.

[5] *IEC Standard for Power Transformers - Part 18: Measurement of Frequency Response*, IEC 60076-18:2012, July 2012.

[6] X. Jiang and A. M. Gole, "A frequency scanning method for the identification of harmonic instabilities in HVDC systems," in *IEEE Trans. on Power Delivery*, vol. 10, no. 4, pp. 1875-1881, Oct. 1995.

[7] A. M. Kulkarni, M. K. Das, and A. M. Gole,"Frequency scanning analysis of STATCOM-network interactions," *2016 IEEE 6th International Conference on Power Systems (ICPS)*, IEEE, 2016.

[8] M. Sahni, D. Muthumuni, B. Badrzadeh, A. Gole and A. Kulkarni, "Advanced screening techniques for sub-synchronous interaction in wind farms," *PES T&D 2012*, Orlando, FL, USA, 2012, pp. 1-9.

[9] M. Bagheri, M. S. Naderi, and T. Blackburn, "Advanced transformer winding deformation diagnosis: moving from off-line to on-line," *IEEE Trans. on Dielectrics and Electrical Insulation*, vol. 19, no. 6, pp. 1860–1870, Dec. 2012.

[10] F. Nasirpour, M. H. Samimi, and H. Mohseni, "Evaluation of online techniques utilized for extracting the transformer transfer function," *S. Iranica Trans. on CSE&EE(D)*, vol. 26, pp. 3582–3591, Dec. 2019.

[11] R. Wimmer and K. Feser, "Calculation of the transfer function of a power transformer with online measuring data," *Prace Naukowe Instytutu Podstaw Elektrotechniki i Elektrotechnologii Politechniki Wrocławskiej. Konferencje*, vol. 40, no. 15, pp. 86–90, 2004.

[12] L. T. Coffeen, "System and method for on-line impulse frequency response analysis," U.S. Patent 6 549 017, Apr. 15, 2003.

[13] K. Dey and A. M. Kulkarni, "Analysis of the passivity characteristics of synchronous generators and converter-interfaced systems for grid interaction studies," *International Journal of Electrical Power and Energy Systems* 129, (2021).

[14] H. K. Høidalen, B. A. Mork, F. Gonzalez, D. Ishchenko, and N. Chiesa, "Implementation and verification of the hybrid transformer model in ATPDraw," *Electric Power Systems Research*, vol. 79, no. 3, pp. 454–459, Mar. 2009.

[15] G. Rêma, D. de Souza, C. Vasques, R. de Azevedo, G. Luz, B. Bonatto, A. de Lima, R. d. S. Delgado, H. Martins, and D. Sixel, "Black-box modeling of power transformers at high frequencies," *Proc. of IPST conference*, June 2019.

[16] J. R. Marti, "Accurate modelling of frequency-dependent transmission lines in electromagnetic transient simulations," *IEEE Trans. on Power Apparatus and Systems*, vol. PAS-101, no. 1, pp. 147–157, Jan. 1982.

[17] S. Murthy and A. Santhakumar, *Transmission Line Structures*, McGraw-Hill, 1990, pp. 27-57.

[18] MATLAB, *Zero-phase digital filtering*. Accessed on Oct. 15, 2020. [Online] Available: https://in.mathworks.com/help/signal/ref/filtfilt.html

[19] Schauder C. and Mehta H.,"Vector analysis and control of advanced static VAR compensators," *In IEE Proceedings CGT& D)*, vol. 140, no. 4, pp. 299-306), IET Digital Library, July 1993.

[20] W. Ren and E. Larsen, "A refined frequency scan approach to sub-synchronous control interaction (SSCI) study of wind farms," in *IEEE Trans. on Power Systems*, vol.31, no.5, pp. 3904-3912, Sep.2016.

[21] M. K. Das and A. M. Gole, "Dependence of frequency response of a STATCOM on the magnetizing reactance of its interfacing transformer," 2018 20th *National Power Systems Conference (NPSC)*, Tiruchirappalli, India, 2018.

[22] "First benchmark model for computer simulation of subsynchronous resonance," in *IEEE Trans. on Power Apparatus and Systems*, vol. 96, no. 5, pp. 1565-1572, Sept. 1977.

[23] Padiyar, K. R., *Analysis of subsynchronous resonance in power systems,* Springer Science & Business Media, 2012.

[24] F. A. Netshiongolwe and J. M. van Coller, "Electrical stress monitoring of distribution transformers using bushing embedded capacitive voltage dividers and Rogowski coils," in *Proc. of IPST*, June 2015.

[25] R. J. Murphy, "Disturbance recorders trigger detection and protection," *IEEE Comp. Applications in Power*, vol. 9, no. 1, pp. 24–28, Jan. 1996.